Large Hydroazaacene Diimides: Synthesis, Tautomerism, Halochromism, and Redox-switchable NIR Optics

Supplementary Information

*Kang Cai, Qifan Yan, and Dahui Zhao**

Beijing National Laboratory for Molecular Sciences, Department of Applied Chemistry and the Key Laboratory of Polymer Chemistry and Physics of the Ministry of Education, College of Chemistry, Peking University, Beijing 100871, China
Email: dhzhao@pku.edu.cn

Table of contents

I. Synthetic Procedures and Characterization Data •••••••••••••••••••••••••••••••••• S2

II. Optical Spectra ••• S5

III. Computational Studies •• S8

IV. Electrochemical Characterizations ••••••••••••••••••••••••••••••••••••••• S12

References ••S14

Copies of ^{1}H and ^{13}C NMR Spectra •••••••••••••••••••••••••••••••••••• S15

I. Synthetic Procedures and Characterization Data

General Methods. Chemicals were used as received unless otherwise indicated. All oxygen or moisture sensitive reactions were performed under nitrogen atmosphere using the standard Schlenk method. Reagent-grade tetrahydrofuran (THF) was distilled over sodium and benzophenone. ^{1}H and ^{13}C NMR spectra were recorded on Mercury plus 300 (300 MHz), Bruker Avance 400 (400 MHz), or Bruker-500 MHz Avance III (500 MHz), using $CDCl_3$ as the solvent unless otherwise noted. Chemical shifts in ^{1}H NMR spectra were reported in parts per million (ppm) with TMS (0 ppm) or residual solvent resonance (7.26 ppm for $CDCl_3$ and 3.62 ppm for THF-d_8) as the reference. TMS (0 ppm) or $CDCl_3$ (77.0 ppm) was the reference for ^{13}C NMR spectra. MALDI-TOF mass spectra were recorded on an ABI 4800 Plus MALDI TOF/TOF™ Analyzer. HR-ESI mass spectra were recorded on a Bruker Apex IV Fourier transformation mass spectrometer. Elemental analyses were performed using a German Vario EL III elemental analyzer.

Synthesis route

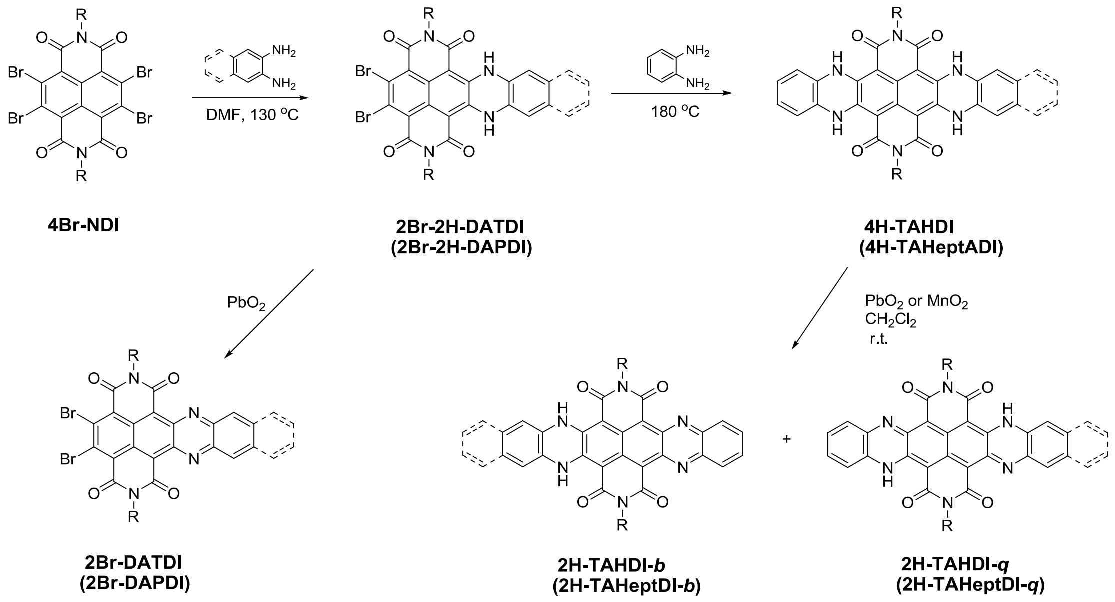

2Br-2H-DATDI: A mixture of **4Br-NDI**[1] (456 mg, 0.40 mmol) and benzene-1,2-diamine (65 mg, 0.60 mmol) in DMF (10 mL) was heated at 130 °C for 1 h. After depletion of **4Br-NDI**, as monitored by TLC, the reaction mixture was diluted with petroleum ether (50 ml), and then washed with water three times to remove DMF. The organic solution was dried over Na_2SO_4 and then solvents were removed *in vacuo*. The crude product was purified with column chromatography over silica gel, eluted with dichloromethane/petroleum ether (DCM/PE=1/4, v/v) to afford **2Br-2H-DATDI** as a dark purple solid (421 mg, 97%). ^{1}H NMR ($CDCl_3$, 300 MHz) δ 13.06 (s, 2H), 7.03-7.00 (m, 2H), 6.84-6.81 (m, 2H), 4.04 (d, J = 7.2 Hz, 4H), 1.92 (br, 2H), 1.23-1.10 (m, 64H), 0.88-0.84 (m, 12H). ^{13}C NMR ($CDCl_3$, 100 MHz) δ 164.5, 160.0, 141.6, 127.1, 126.8, 126.4, 121.1, 116.5, 94.9, 44.9, 36.2, 32.0, 31.7, 30.2, 29.8, 29.7, 29.6, 29.4, 26.4, 22.7, 14.1.

2Br-DATDI: A mixture of **2Br-2H-DATDI** (80 mg, 0.073 mmol) and PbO_2 (300 mg, 1.25 mmol) in DCM (4 mL) was stirred at 50 °C for 24 h, while the color of the solution turned from purple to yellow. Upon depletion of **2Br-2H-DATDI**, as monitored by TLC, the solution was cooled and filtered to remove the insoluble materials. The solution was dried over anhydrous Na_2SO_4 and then concentrated *in vacuo*. The residue was purified with column chromatography over silica gel, eluted with DCM to afford **2Br-DATDI** as a yellow solid (74 mg, 93%). ^{1}H NMR ($CDCl_3$, 300 MHz) δ 8.43-8.40 (m, 2H), 8.02-7.99 (m, 2H), 4.31 (d, *J* = 7.2 Hz, 4H), 2.12 (br, 2H), 1.39-1.22 (m, 64H), 0.88-0.82 (m, 12H). ^{13}C NMR ($CDCl_3$, 100 MHz) δ 161.0, 160.0, 145.0, 138.9, 137.4, 133.8, 130.7, 126.4, 126.3, 121.2, 46.2, 36.6, 31.9, 31.7, 30.2, 29.73, 29.66, 29.6, 29.4, 22.7, 14.1. HRMS (ESI): Calcd. for $C_{60}H_{87}N_4O_4Br_2$ 1087.5074 (M + H$^+$); Found: 1087.5070. Elem. Anal.: Calcd. for $C_{60}H_{86}N_4O_4Br_2$: C, 66.29; H, 7.97; N, 5.15. Found: C, 66.47; H, 8.02; N, 5.16.

2Br-2H-DAPDI: A mixture of **4Br-NDI** (456 mg, 0.40 mol), naphthylene-2,3-diamine (90 mg, 0.57 mmol) and K_2CO_3 (120 mg, 0.87 mmol) in DMF (10 mL) was heated at 100 ^{o}C for 2 h. After cooled to r.t., the reaction mixture was diluted with PE (50 mL), washed with water (x3), and then dried over anhydrous Na_2SO_4. After solvents were removed *in vacuo*, the residue was purified with column chromatography over silica gel, eluted with DCM/PE (1:3, v/v) to afford **2Br-2H-DAPDI** as a dark purple solid (390 mg, 87%). ^{1}H NMR ($CDCl_3$, 300 MHz) δ 12.93 (s, 2H), 7.40-7.38 (m, 2H), 7.20-7.18 (m, 2H), 6.93 (s, 2H), 3.93 (d, *J* = 7.2 Hz, 4H), 1.90 (br, 2H), 1.23 (m, 64H), 0.87-0.83 (m, 12H). ^{13}C NMR ($CDCl_3$, 75 MHz) δ 164.7, 160.1, 140.1, 131.6, 127.8, 126.8, 126.4, 125.9, 125.8, 121.7, 112.5, 96.0, 44.9, 36.3, 31.9, 31.6, 30.2, 29.8, 29.7, 29.6, 29.4, 26.4, 22.7, 14.1. HRMS (ESI): Calcd. for $C_{64}H_{90}Br_2N_4O_4$, 1138.5308 (M$^+$); Found: 1138.5310.

2Br-DAPDI: A mixture of **2Br-2H-DAPDI** (15 mg, 0.013 mmol) and PbO_2 (100 mg, 0.42 mmol) in 1,2-dichloroethane (2 mL) was stirred reflux for 1 h. The color of the solution turned from purple to deep yellow. After **2Br-2H-DAPDI** was completely consumed, as monitored by TLC, the reaction mixture was filtered to remove the insoluble materials. The filtrate was dried over anhydrous Na_2SO_4 and then condensed *in vacuo*. The residue was purified with column chromatography over silica gel, eluted with DCM to afford **2Br-DAPDI** as a yellow solid (9.0 mg, 60%). ^{1}H NMR ($CDCl_3$, 300 MHz) δ 9.03 (s, 2H), 8.09-8.06 (m, 2H), 7.55-7.52 (m, 2H), 4.33 (d, *J* = 7.5 Hz, 4H), 2.17-2.13 (m, 2H), 1.59-1.22 (m, 64H), 0.87-0.82 (m, 12H). ^{13}C NMR ($CDCl_3$, 75 MHz) δ 161.2, 160.2, 141.1, 139.3, 137.9, 137.3, 129.2, 129.0, 128.6, 127.1, 126.4, 121.3, 46.3, 36.7, 32.0, 31.7, 30.2, 29.7, 29.4, 26.4, 22.7, 14.2. HRMS (ESI): Calcd. for $C_{64}H_{89}Br_2N_4O_4$, 1137.5230 (M + H$^+$), Found: 1137.5223.

4H-TAHDI: A mixture of **4Br-NDI** (342 mg, 0.30 mmol) and benzene-1,2-diamine (3.1 g, 29 mmol) was heated at 180 ^{o}C under N_2 atmosphere for 2 d. After water (20 mL) and MeOH (20 mL) being added, and the resultant mixture was extracted with PE for four times. The combined organic layers were dried over anhydrous Na_2SO_4 and then condensed *in vacuo*. The crude product was purified with column chromatography over silica gel, eluted with DCM/PE (1:5, v/v) to afford **4H-TAHDI** as a deep green solid (87 mg, 28%). ^{1}H NMR ($CDCl_3$, 300 MHz) δ 11.02 (br, 4H), 6.53 (br, 4H), 6.29 (br, 4H), 3.77 (d, *J* = 7.2Hz, 4H), 1.77 (br, 2H), 1.22 (m, 64H), 0.87-0.83 (m, 12H). ^{13}C NMR ($CDCl_3$, 75 MHz) δ 165.2, 138.1, 129.7, 123.7, 117.6, 114.4, 98.6, 43.6, 36.2, 31.98, 31.80, 31.6, 30.2, 29.7, 29.4, 26.5, 22.7, 14.1. HRMS (ESI): Calcd. for $C_{66}H_{94}N_6O_4$ (M$^+$): 1034.7331; Found: 1034.7331. Elem. Anal.: Calcd. for $C_{66}H_{94}N_6O_4$: C, 76.55; H, 9.15; N, 8.12. Found: C, 76.34; H, 9.12; N, 8.09.

2H-TAHDI-*b*/2H-TAHDI-*q*: A mixture of **4H-TAHDI** (20 mg, 0.019 mmol) and MnO_2 (100 mg, 1.1 mmol) in DCM (5 mL) was stirred at room temperature for 1 h. The color of the solution turned from green to deep blue. After **4H-TAHDI** was completely consumed, as monitored by TLC, the reaction mixture was filtered. The filtrate was dried over anhydrous Na_2SO_4 and then condensed in *vacuo*. The residue was purified with column chromatography over silica gel, eluted with DCM to afford **2H-TAHDI-*b*/2H-TAHDI-*q*** as a deep blue solid (19 mg, 96%, a mixture of isomers).

2H-TAHDI-*b*: ^{1}H NMR ($CDCl_3$, 20 ^oC) δ 14.46 (s, 2H), 8.25-8.23 (m, 2H), 7.73-7.70 (m, 2H), 6.95-6.92 (m, 2H), 6.87-6.84 (m, 2H), 4.23-4.19 (m, 4H), 2.13 (br, 2H), 1.39-1.21 (m, 64H), 0.87-0.83 (m, 12H). **2H-TAHDI-*q***: ^{1}H NMR ($CDCl_3$, 20 ^oC) δ 16.77 (s, 2H), 8.08-8.06 (m, 2H), 7.49-7.27 (m, 6H), 4.23-4.19 (m, 4H), 2.13 (br, 2H), 1.39-1.21 (m, 64H), 0.87-0.83 (m, 12H).
2H-TAHDI-*b*/2H-TAHDI-*q*: ^{13}C NMR ($CDCl_3$, 75 MHz, 20 ^oC) δ 165.9, 165.6, 160.3, 159.9, 146.0, 145.3, 141.1, 140.6, 140.5, 137. 3, 136.8, 131.5, 131.1, 130.4, 130.2, 127.9, 126.8, 126.5, 125.9, 117.8, 114.2, 106.9, 94.7, 93.2, 44.8, 36.1, 36.0, 31.9, 31.7, 30.3, 29.7, 29.67, 29.4, 26.5, 22.7, 14.1. HRMS (ESI): Calcd. for $C_{66}H_{93}N_6O_4$ ($M+H^+$): 1033.7253; Found: 1033.7233. Elem. Anal.: Calcd. for $C_{66}H_{92}N_6O_4$: C, 76.63; H, 9.06; N, 8.12. Found: C, 76.63; H, 9.10; N, 8.01.

Procedure for the reduction of **2H-TAHDI** to **4H-TAHDI**: A mixture of **2H-TAHDI** (5 mg, 0.0047 mmol), $NaBH_4$ (5 mg, 0.13 mmol) and $CoCl_2{\cdot}6H_2O$ (0.1 mg) in $CHCl_3$/EtOH (1 mL + 1 mL) was stirred at room temperature. The color of the solution turned from deep blue to green very soon. The reaction was monitored by absorption spectra, which showed that **2H-TAHDI** was completely converted into **4H-TAHDI** in 10 minutes.

4H-DAHeptDI: A mixture of **2Br-2H-DAPDI** (228 mg, 0.020 mmol) and benzene-1,2-diamine (4.0 g, 0.037 mol) was heated at 180 ^oC under N_2 atmosphere for 2 d. After water (20 mL) and MeOH (20 mL) being added, the reaction mixture was extracted with PE for four times. The combined organic layers were dried over anhydrous Na_2SO_4 and then condensed *in vacuo*. The residue was purified with column chromatography of silica gel, eluted with DCM/PE (1:5, v/v) to afford **4H-DAHeptDI** as a deep green solid (71 mg, 31%). ^{1}H NMR ($CDCl_3$, 300 MHz) δ 11.15 (br, 4H), 7.19-7.16 (m, 2H), 6.88 (br, 2H), 6.49 (br, 2H), 6.40 (br, 2H), 6.21 (br, 2H), 3.84 (d, J = 7.2Hz, 4H), 1.87 (br, 2H), 1.24 (m, 64H), 0.87-0.83 (m, 12H). ^{13}C NMR ($CDCl_3$, 100 MHz) δ 165.2, 165.1, 138.7, 135.4, 131.5, 129.2, 125.8, 124.5, 123.7, 117.6, 114.5, 108.9, 99.6, 43.8, 36.3, 32.0, 31.7, 30.4, 30.24, 30.17, 30.1, 29.9, 29.80, 29.75, 29.5, 29.4, 26.5, 22.7, 14.1. MALDI-TOF MS: Calcd. for $C_{70}H_{96}N_6O_4$: 1084.7 (M^+), Found: 1084.9. Elem. Anal.: Calcd. for $C_{70}H_{96}N_6O_4$: C, 77.45; H, 8.91; N, 7.74. Found: C, 77.34; H, 9.03; N, 7.38.

2H-DAHeptDI: A mixture of **4H-DAHeptDI** (20 mg, 0.018 mmol) and MnO_2 (300 mg, 3.3 mmol) in DCM (5 mL) was stirred at room temperature for 1 h. The color of the solution was observed to turn from green to deep blue. After **4H-TAHDI** was completely consumed, as monitored by TLC, the reaction mixture was filtered to remove the insoluble. The filtrate was dried over anhydrous Na_2SO_4 and then condensed *in vacuo*. The residue was purified with column chromatography of silica gel, eluted with DCM to afford **2H-DAHeptDI** as a deep blue solid (18 mg, 90%). ^{1}H NMR ($CDCl_3$, 400 MHz, the major component of the mixture) δ 14.45 (s, 2H), 8.19-8.17 (m, 2H), 7.64-7.61 (m, 2H), 7.53-7.50 (m, 2H), 7.33 (s, 2H), 7.24-7.21 (m, 2H), 4.28 (d, J = 7.6Hz, 4H), 2.18 (s, br 2H), 1.60-1.21 (m, 64H), 0.85-0.79 (m, 12H). ^{13}C NMR ($CDCl_3$, 50 MHz) δ 165.7, 160.3, 142.3, 140.2, 131.5, 130.4, 130.1, 126.9, 126.6, 124.8, 114.9, 113.8, 111.9, 111.5 , 95.4, 44.9, 38.6, 36.2, 33.7, 31.9, 30.3, 29.7, 29.4, 26.7, 22.6, 14.1. MALDI-TOF MS: Calcd. for $C_{70}H_{94}N_6O_4$: 1082.7 (M^+), Found: 1082.7. Elem. Anal.: Calcd. for $C_{66}H_{92}H_6O_4$: C, 77.59; H, 8.74; N, 7.76. Found: C, 77.33; H, 8.95; N, 7.42.

II. Optical Spectra

UV-vis absorption spectra of the compounds were recorded on a Hitachi U-4100 spectrophotometer using 1-cm quartz cell. The solvents, DCM, $CHCl_3$ and THF, were distilled over CaH_2 or Na prior to use.

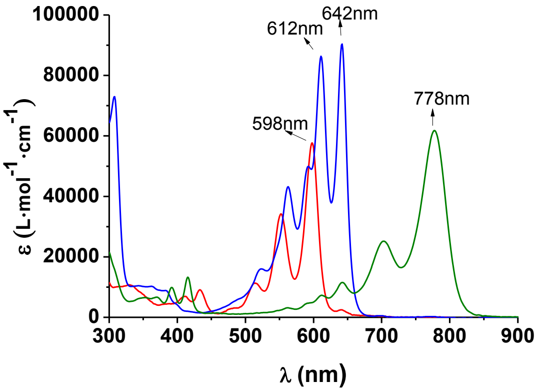

Figure S1. Absorption spectra of **2Br-2H-DATDI** (red), **2H-TAHDI** (blue), and **4H-TAHDI** (green) in CH_2Cl_2.

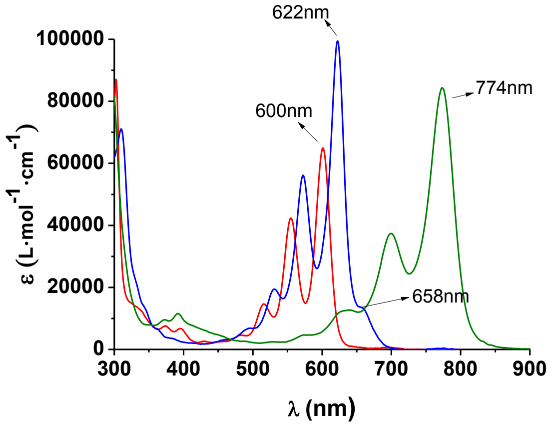

Figure S2. Absorption spectra of **2Br-2H-DAPDI** (red), **2H-TAHeptDI** (blue), and **4H-TAHeptDI** (green) in CH_2Cl_2.

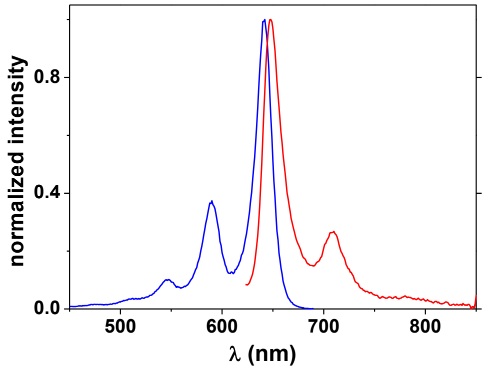

Figure S3. Fluorescence excitation (blue line, with emission monitored at 710 nm) and emission (red line, excited at 590 nm where both tautomers absorb) spectra of 2H-TAHDI in CH_2Cl_2.

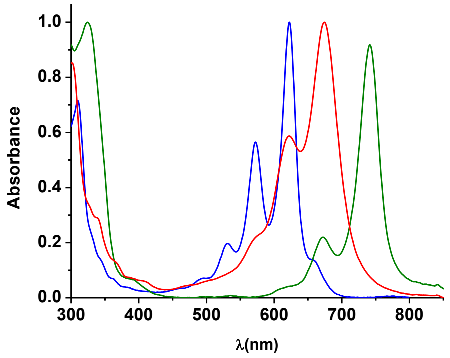

Figure S4. Absorption spectra of **2H-TAHeptDI** in DCM (blue), HOAc (red), H_2SO_4 (green).

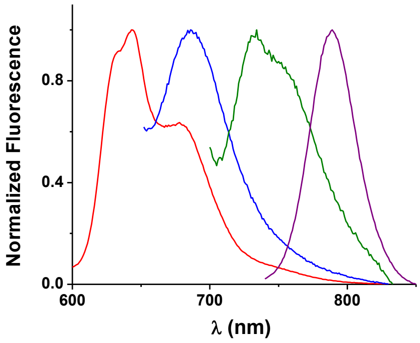

Figure S5. Emission spectra of **2H-TAHeptDI** in DCM (red), HOAc (blue), H_2SO_4 (green) and **4H-TAHeptDI** in DCM (purple).

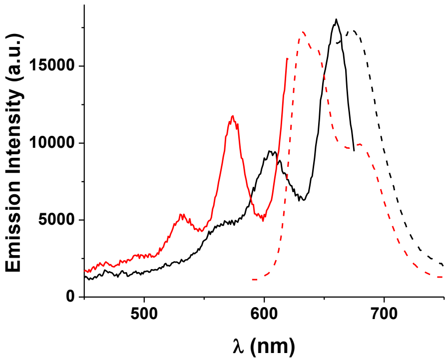

Figure S6. Fluorescence excitation spectra with emission monitored at 685 nm (black solid) and 630 nm (red solid) and emission spectra excited at 575 nm (red dashed) and 650 nm (black dashed) of **2H-TAHeptDI** in $CHCl_3$.

Table S1. Summary of optical absorption and emission properties

compd.	Absorption maximum λ_{abs} (nm)	Emission maximum λ_{fl} (nm)	Fluorescence quantum yield
2H-TAHDI[a]	611/642	647	8.25[d]
(3H-TAHDI)$^+$[b]	665	688	13.60
(4H-TAHDI)$^{2+}$[c]	724	741	5.30
4H-TAHDI[a]	778	793	2.85
2H-TAHeptDI[a]	621/661	642	1.28[e]
(3H-TAHeptDI)$^+$[b]	675	685	0.40
(4H-TAHeptDI)$^{2+}$[c]	742	733	0.01
4H-TAHeptDI[a]	774	789	1.32

[a] In DCM; [b] in HOAc; [c] in H_2SO_4; [d] the quantum yield was estimated for the tautomer mixture, and true quantum yield of the more emissive 2H-TAHDI-*q* should be approximately doubled; [e] the quantum yield was estimated for the tautomer mixture.

III. Computational Studies

The geometry of the molecules was optimized with Density Functional Theory (DFT) using B3LYP hybrid functional[2] with a basis set limited to 6-31g+d. Molecular orbital shapes and energies were obtained at optimized geometries. TD-DFT calculation was performed at optimized geometries with theory level at B3LYP/6-31g+d. NICS indexes at the ring centers was calculated at B3LYP/6-31g+d level. Quantum-chemical calculation was performed with the Gaussian03[3] package and the orbital pictures were prepared using Gaussview.[4] All long alkyl substituents were replaced with methyl groups in calculations.

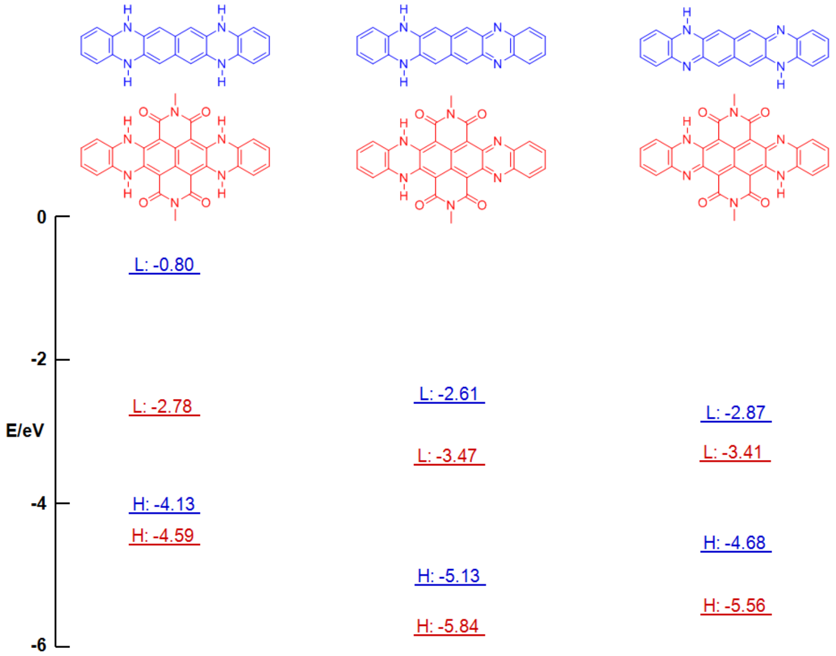

Figure S7. B3lyp/6-31g+d calculated energy levels of frontier molecular orbitals of the dihydro- and tetahydrotetraazahexacene (in blue) and their diimide derivatives (in red). (Unit: eV; H: HOMO; L: LUMO)

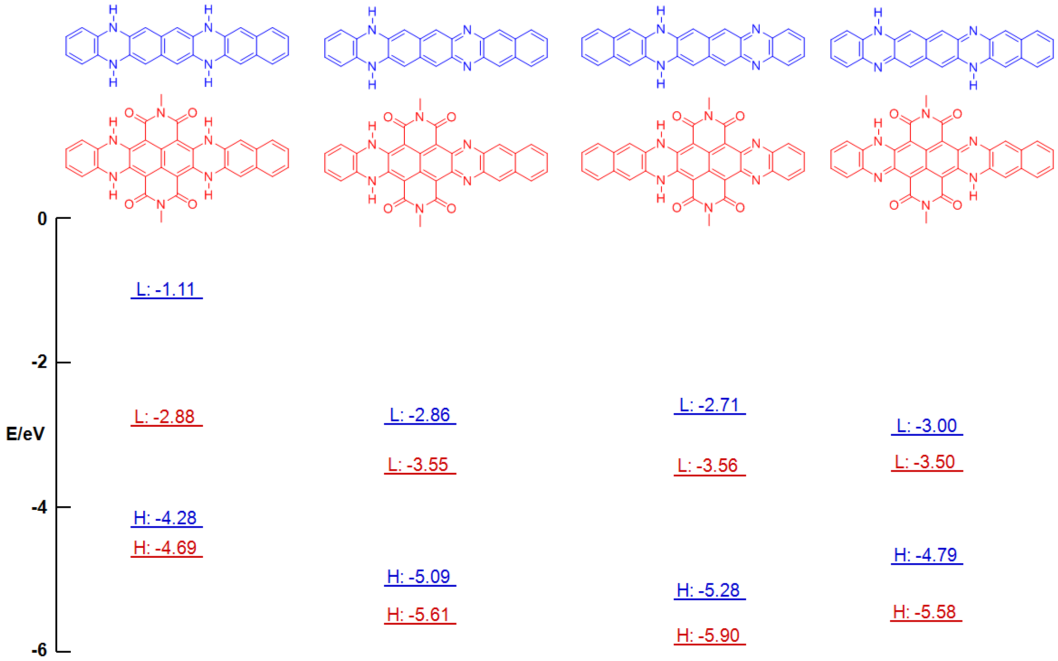

Figure S8. B3lyp/6-31g+d calculated energy levels of frontier molecular orbitals of the dihydro- and tetahydrotetraazaheptacene (in blue) and their diimide derivatives (in red). (Unit: eV; H: HOMO; L: LUMO)

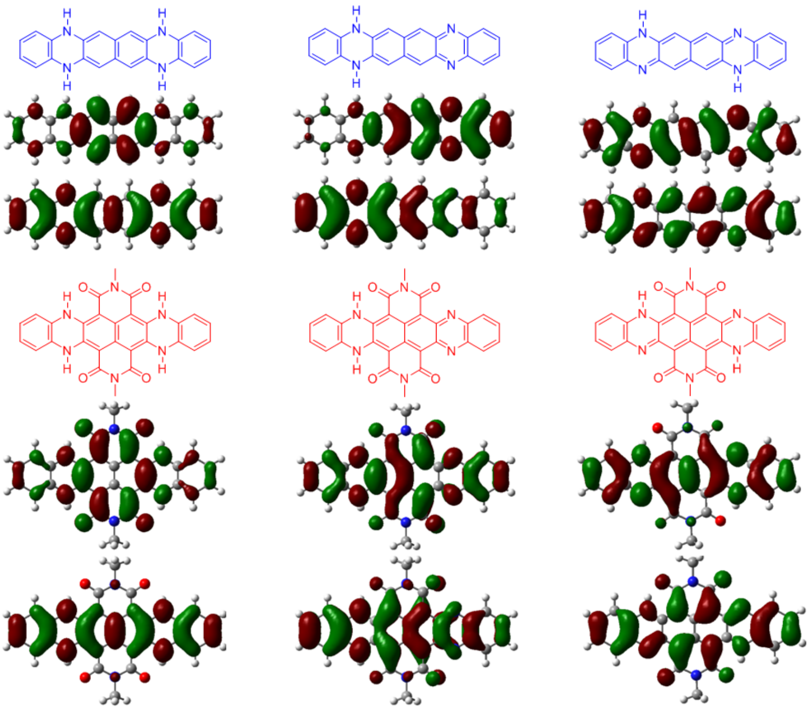

Figure S9. DFT calculated frontier molecular orbitals of tetrahydrotetraazahexacene, benzenoid and quinonoid tautomers of dihydrotetraazahexacene, and those of their corresponding diimide derivatives (LUMO: upper; HOMO: lower).

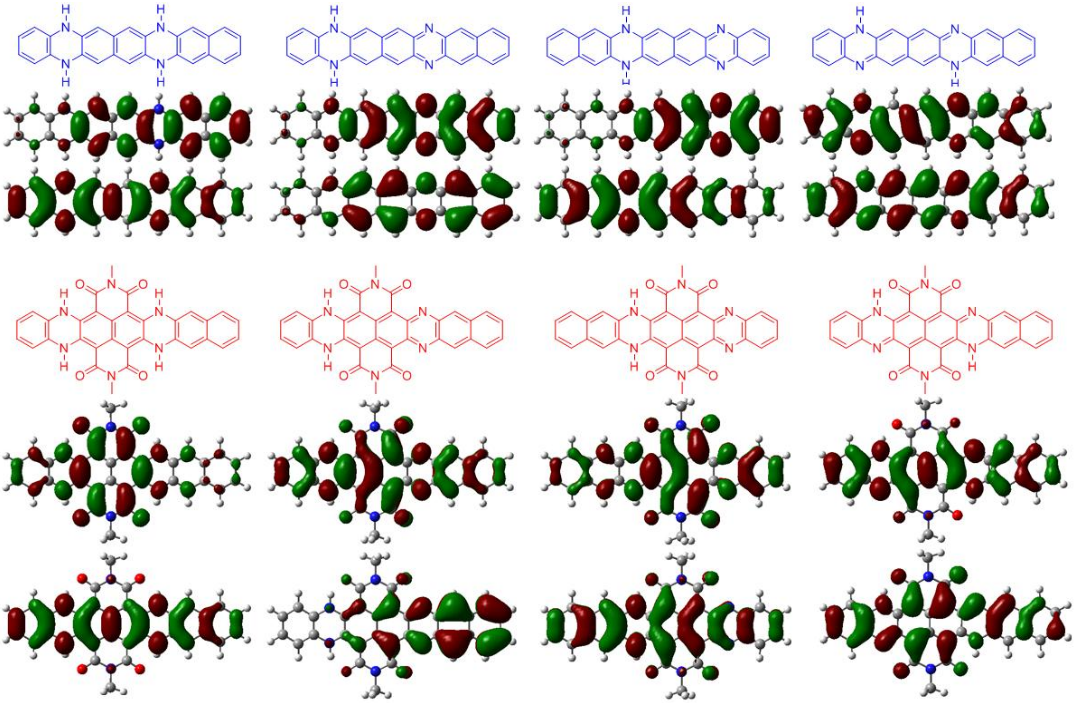

Figure S10. DFT calculated frontier molecular orbitals of tetrahydrotetraazaheptacene, benzenoid and quinonoid tautomers of dihydrotetraazaheptacene, and those of their corresponding diimide derivatives (LUMO: upper; HOMO: lower).

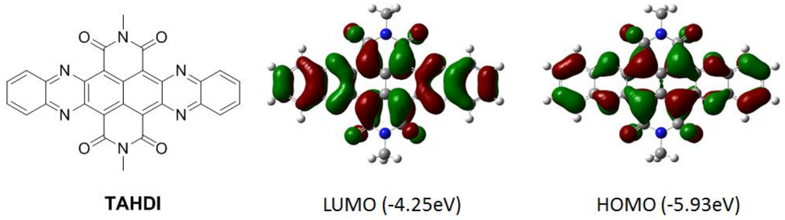

Figure S11. Structure and DFT calculated LUMO and HOMO of TAHDI.

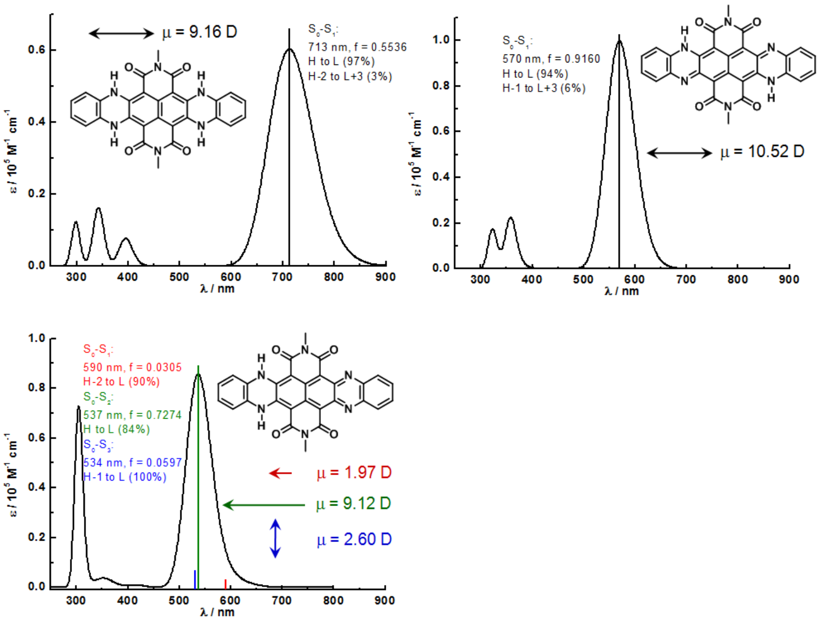

Figure S12. TD-DFT simulated UV-vis spectra with 20 excited states of 4H-TAHDI and different 2H-TAHDI tautomers, with transition energy, oscillator strength (f), assignments, and transition dipole (μ) of low energy transitions as shown (FWHM was set as 1000 cm^{-1}).

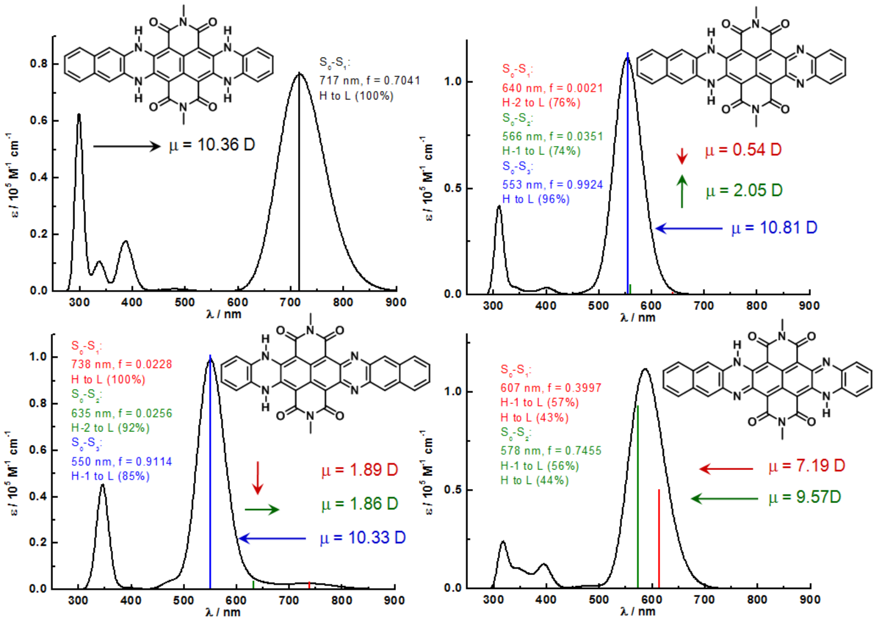

Figure S13. TD-DFT simulated UV-vis spectra with 20 excited states of 4H-TAHeptDI and different 2H-TAHeptDI tautomers, with transition energy, oscillator strength (f), assignments and transition dipole (μ) of low energy transitions as shown (FWHM was set as 1000 cm^{-1}).

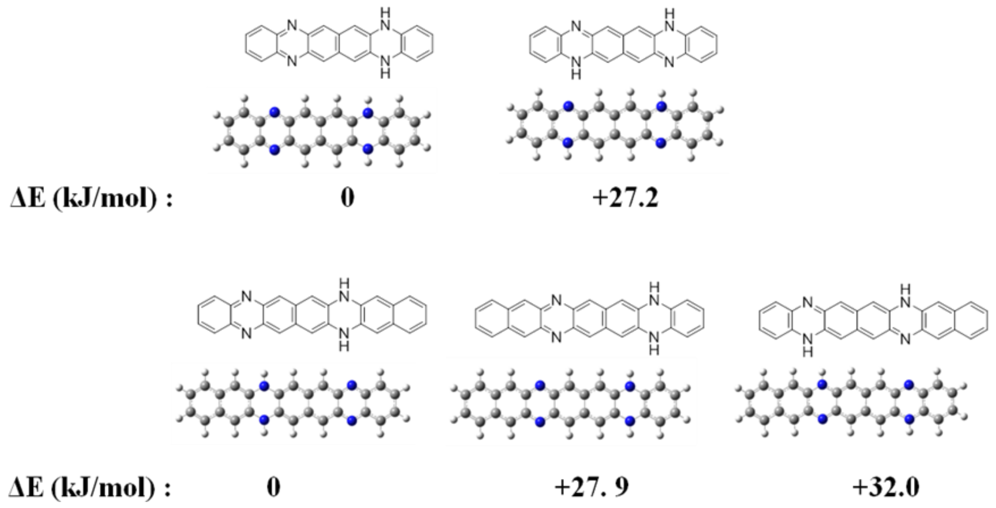

Figure S14. Computed optimized geometries of benzenoid and quinonoid tautomers of **2H-TAH and 2H-TAHept**, with relative total energy values shown.

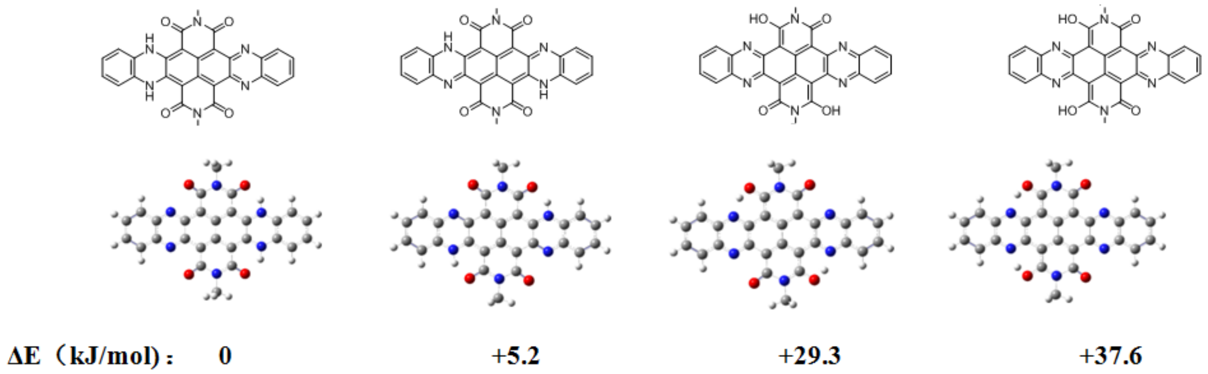

Figure S15. Computed optimized geometries of all possible tautomers of **2H-TAHDI**, with relative total energy values shown.

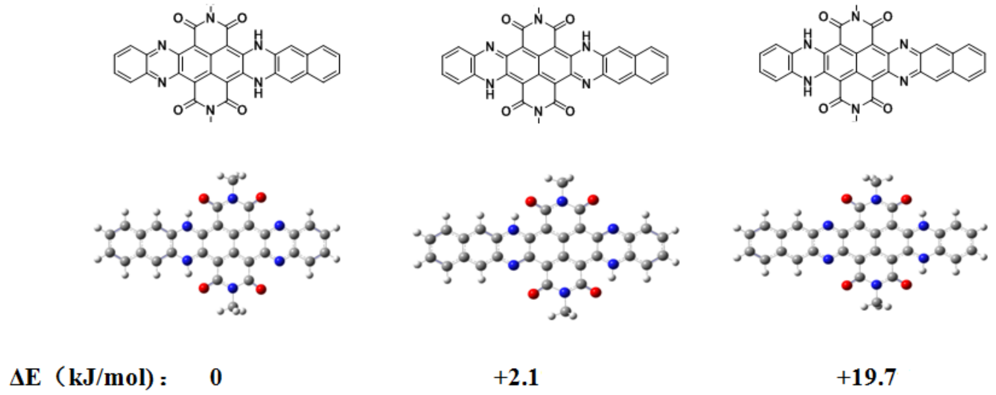

Figure S16. Computed optimized geometries of three possible tautomers of **2H-TAHeptDI**, with relative total energy values shown.

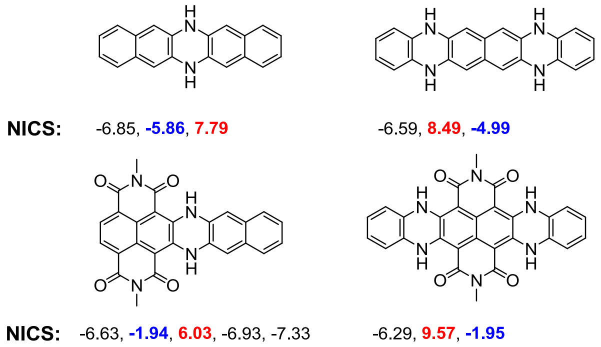

Figure S17. Calculated NICS values (in ppm)[7] of hydroazaacenes and corresponding diimide derivatives

IV. Electrochemical Characterizations

Cyclic voltammetry was performed using BASI Epsilon workstation and measurements were carried out in acetonitrile (for the thin film) or dichloromethane (for the solution) containing 0.1 M n-Bu_4NPF_6 as a supporting electrolyte. Glassy carbon electrode was used as a working electrode and a platinum sheet as a counter electrode. All potentials were recorded versus Ag/AgCl as a reference electrode, and ferrocene/ferrocenium as an external reference. The scan speed was 100 mV s^{-1}. CH_2Cl_2 was freshly distilled over CaH_2 prior to use. The energy level of Fc/Fc^+ is assumed to be -4.8 eV below the vacuum level.[5,6] The LUMO levels of **2Br-DATDI** and **2Br-DAPDI** were estimated from the half-wave potentials of the reduction peaks. The half-wave potential of oxidation peak of Fc was measured to be 0.43 V against Ag/AgCl.

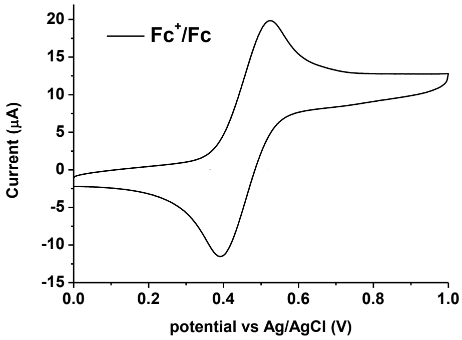

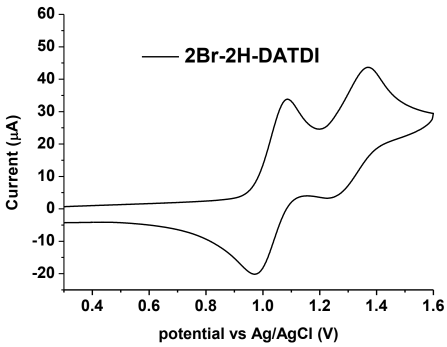

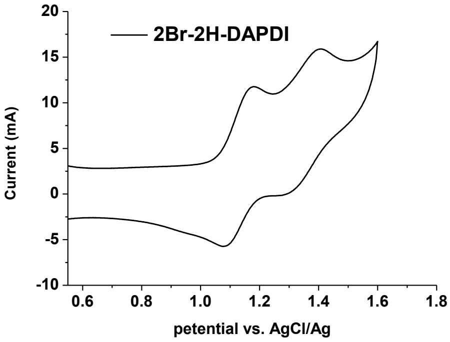

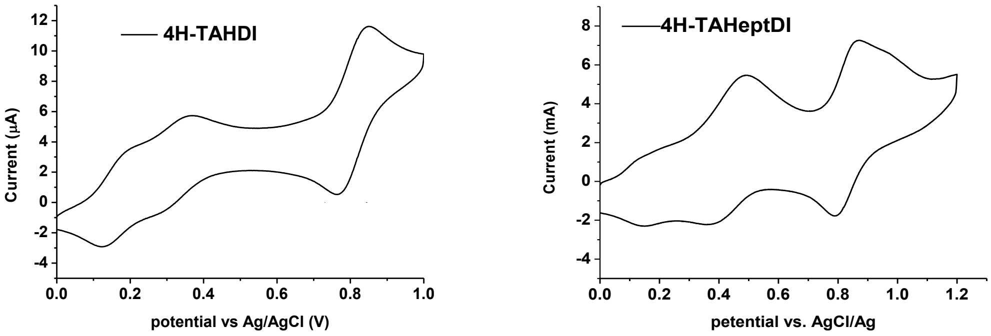

Figure S18. CVs of ferrocene and hydroazaacene diimide derivatives.

Table S2. Summary of electronic data in DCM in comparison with calculated results

Comp.	4H-TAHDI	4H-TAHeptDI	2H-TAHDI-*b*	2H-TAHDI-*q*
λ_{max} abs (nm)	778	774	612	642
HOMO[a] (eV)	-4.49	-4.54	--[d]	--[d]
band gap[b] (eV)	1.43	1.42	--[d]	1.84
LUMO[c] (eV)	-3.06	-3.12	--[d]	--[d]
calcd. HOMO-LUMO energy gap (eV)	1.81	1.81	2.36	2.14
calcd. HOMO (eV)	-4.59	-4.69	-5.53	-5.24
calcd. LUMO (eV)	-2.78	-2.88	-3.17	-3.10

[a] calculated based on CV; [b] estimated from the onset wavelength of the absorption band; [c] estimated based on the above band gap and HOMO data; [d] unable to determine since the absorption spectra and CV of 2H-TAHDI-*b* and 2H-TAHDI-*q* were overlapped for coexisting tautomers.

References

1. Gao, X.; Qiu, W.; Yang, X.; Liu, Y.; Wang, Y.; Zhang, H.; Qi, T.; Liu, Y.; Lu, K.; Du, C.; Shuai, Z.; Yu, G.; Zhu, D. *Org. Lett.* **2007**, *9*, 3917.

2. (a) Becke, A. D. *Phys. Rev. A* **1988**, *38*, 3098. (b) Lee, C.; Yang, W.; Parr, G. G. *Phys. Rev. B* **1988**, *37*, 785.

3. Frisch, M. J.; Trucks, G. W.; Schlegel, H. B.; Scuseria, G. E.; Robb, M. A.; Cheeseman, J. R.; Montgomery, J. A. Jr.; Vreven, T.; Kudin, K. N.; Burant, J. C.; Millam, J. M.; Iyengar, S. S.; Tomasi, J.; Barone, V.; Mennucci, B.; Cossi, M.; Scalmani, G.; Rega, N.; Petersson, G. A.; Nakatsuji, H.; Hada, M.; Ehara, M.; Toyota, K.; Fukuda, R.; Hasegawa, J.; Ishida, M.; Nakajima, T.; Honda, Y.; Kitao, O.; Nakai, H.; Klene, M.; Li, X.; Knox, J. E.; Hratchian, H. P.; Cross, J. B.; Adamo, C.; Jaramillo, J.; Gomperts, R.; Stratmann, R. E.; Yazyev, O.; Austin, A. J.; Cammi, R.; Pomelli, C.; Ochterski, J. W.; Ayala, P. Y.; Morokuma, K.; Voth, G. A.; Salvador, P.; Dannenberg, J. J.; Zakrzewski, V. G.; Dapprich, S.; Daniels, A. D.; Strain, M. C.; Farkas, O.; Malick, D. K.; Rabuck, A. D.; Raghavachari, K.; Foresman, J. B.; Ortiz, J. V.; Cui, Q.; Baboul, A. G.; Clifford, S.; Cioslowski, J.; Stefanov, B. B.; Liu, G.; Liashenko, A.; Piskorz, P.; Komaromi, I.; Martin, R. L.; Fox, D. J.; Keith, T.; Al-Laham, M. A.; Peng, C. Y.; Nanayakkara, A.; Challacombe, M.; Gill, P. M. W.; Johnson, B.; Chen, W.; Wong, M. W.; Gonzalez, C.; Pople, J. A. *Gaussian 03*, Revision C.02; Gaussian Inc.: Wallingford CT, 2004.

4. Dennington, R., II; Keith, T.; Millam, J.; Eppinnett, K.; Hovell, W. L.; Gilliland, R. *GaussView*, Version 3.09; Semichem, Inc.: Shawnee Mission, KS, 2003.

5. Pommerehne, J.; Vestweber, H.; Guss, W.; Mahrt, R. F.; Bassler, H.; Porsch, M.; Daub, J. *Adv. Mater.* **1995**, *7*, 551.

6. Sun, Q.; Wang, H.; Yang, C.; Li, Y. *J. Mater. Chem.* **2003**, *13*, 800.

7. a) Krishnan R.; Binkley J. S.; Seeger R.; Pople J. A. *J. Chem. Phys*. **1980**, *72*, 650; b) Chen Z.; Wannere C. S.; Corminboeuf C.; Puchta R.; Schleyer P. von R. *Chem. Rev.* **2005**, *105*, 3842.

Copies of ^{1}H and ^{13}C NMR Spectra

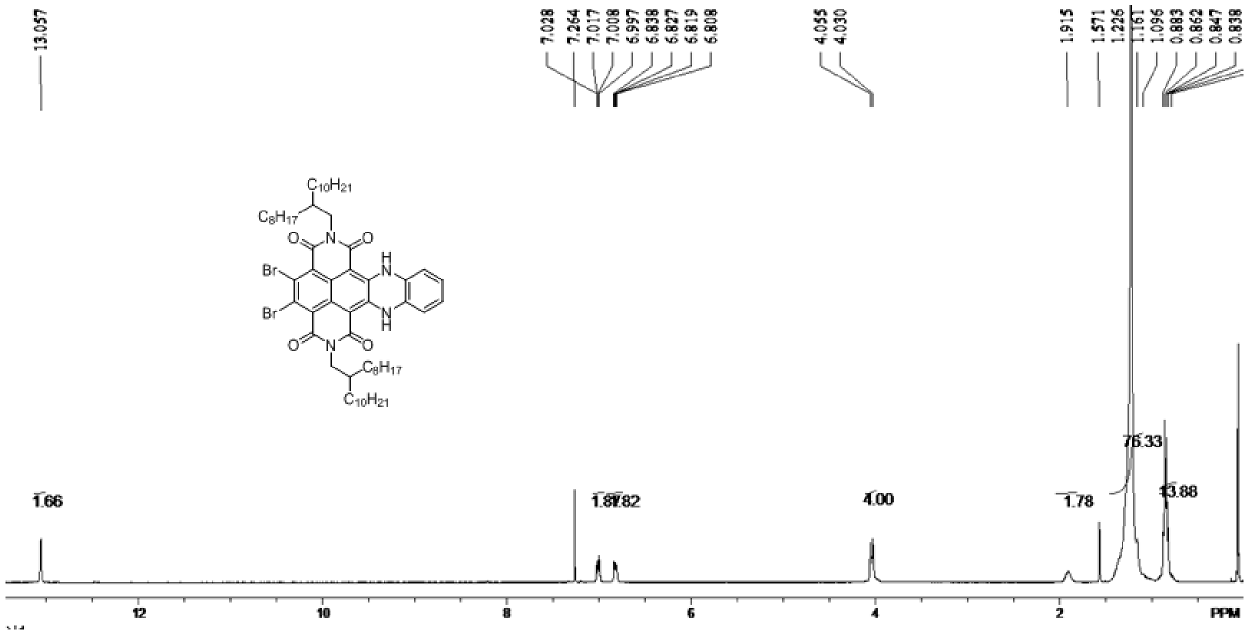

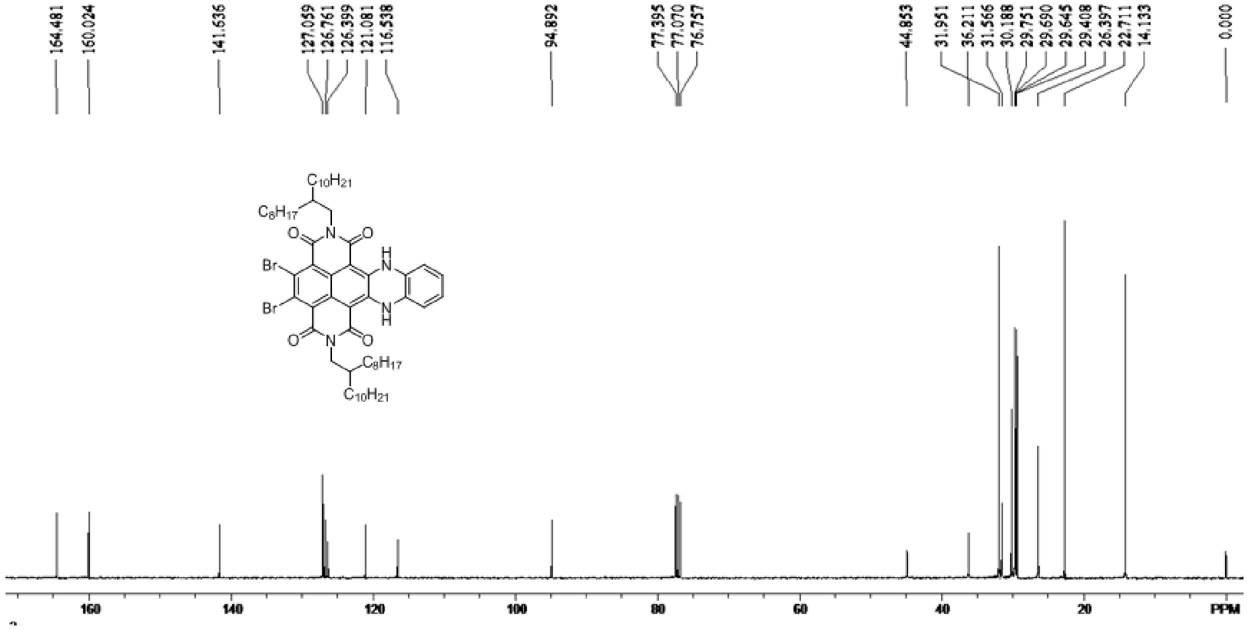

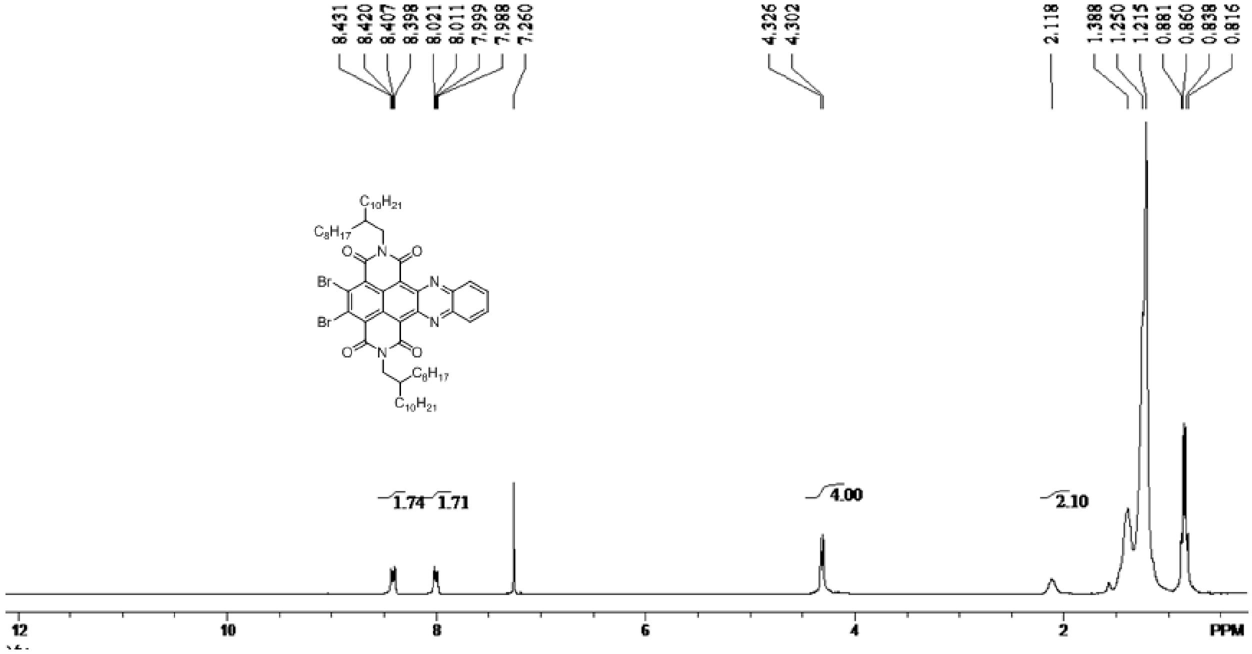
8.431
8.420
8.407
8.398
8.021
8.011
7.999
7.988
7.260
4.326
4.302
2.118
1.388
1.250
1.215
0.881
0.860
0.838
0.816
$C_{10}H_{21}$
C_8H_{17}
O
N
O
Br
Br
N
N
O
N
O
C_8H_{17}
$C_{10}H_{21}$
1.74
1.71
4.00
2.10
12
10
8
6
4
2
PPM

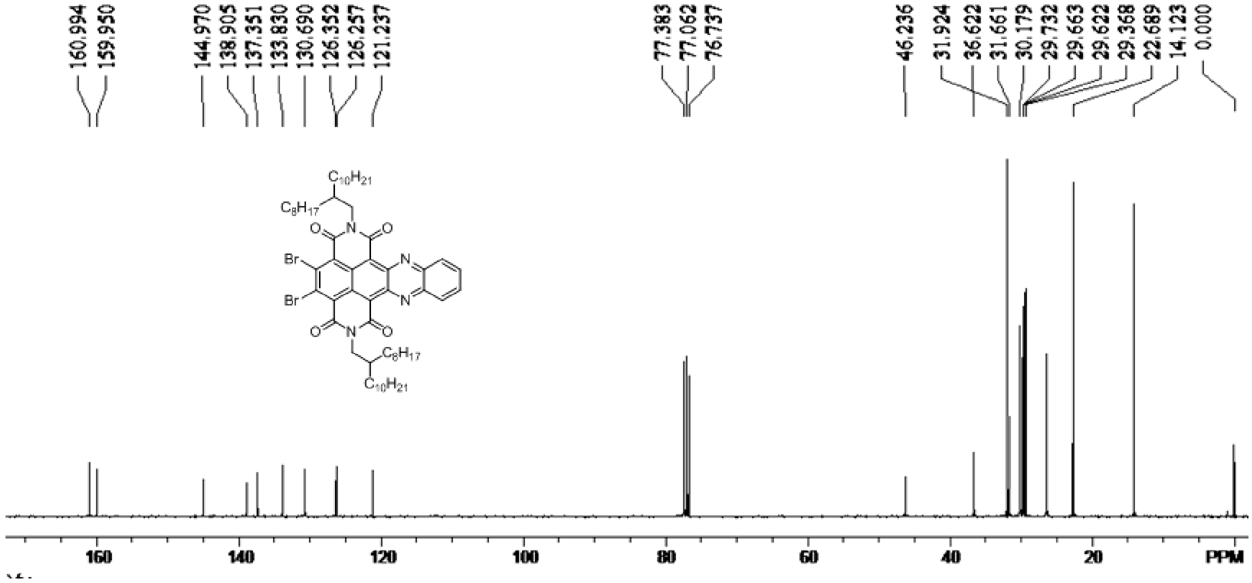
160.994
159.950
144.970
138.905
137.351
133.830
130.690
126.352
126.257
121.237
77.383
77.062
76.737
46.236
31.924
36.622
31.661
30.179
29.732
29.663
29.622
29.368
22.689
14.123
0.000
$C_{10}H_{21}$
C_8H_{17}
O
N
O
Br
Br
N
N
O
N
O
C_8H_{17}
$C_{10}H_{21}$
160
140
120
100
80
60
40
20
PPM

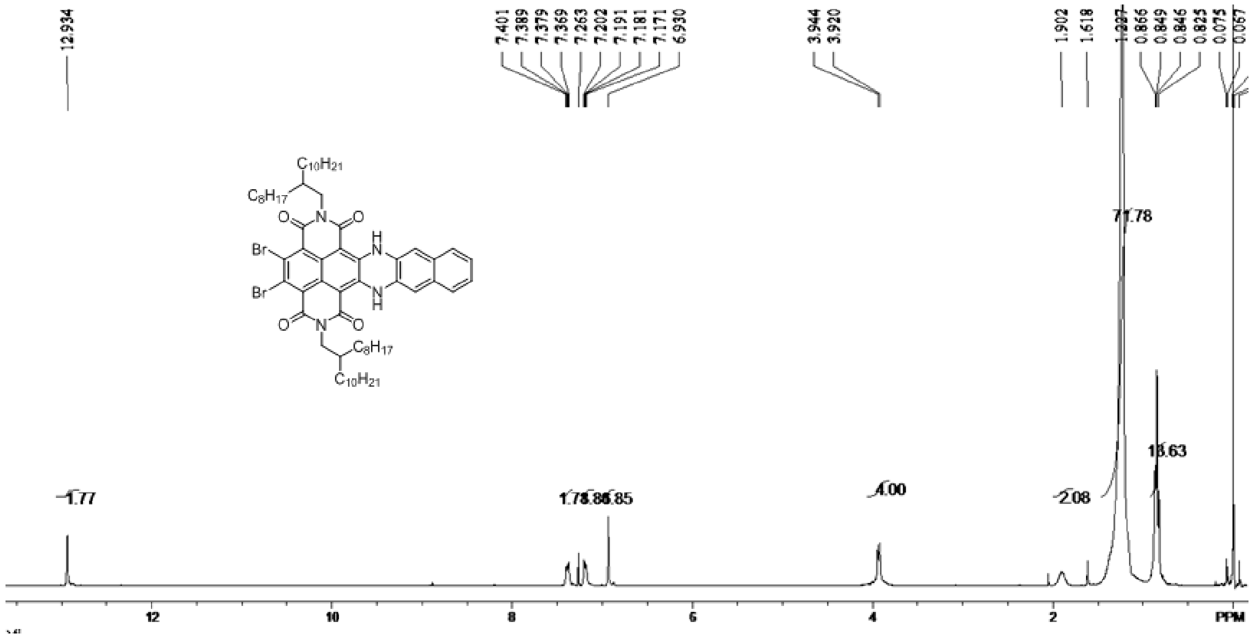
12.934
7.401
7.389
7.379
7.369
7.263
7.202
7.191
7.181
7.171
6.930
3.944
3.920
1.902
1.618
1.287
0.866
0.849
0.846
0.825
0.075
0.067
$C_{10}H_{21}$
C_8H_{17}
O
N
O
H
Br
N
Br
N
H
O
N
O
C_8H_{17}
$C_{10}H_{21}$
71.78
18.63
1.77
1.78
1.86
1.85
4.00
2.08
12
10
8
6
4
2
PPM

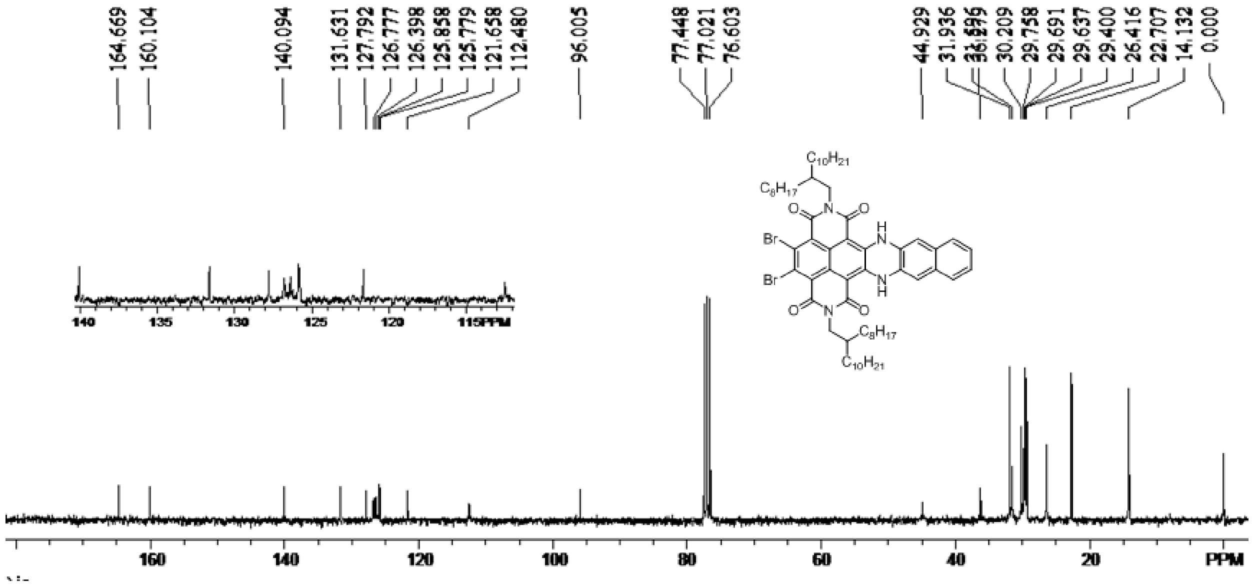
164.669
160.104
140.094
131.631
127.792
126.777
126.398
125.858
125.779
121.658
112.480
96.005
77.448
77.021
76.603
44.929
31.936
31.595
30.209
29.758
29.691
29.637
29.400
26.416
22.707
14.132
0.000
$C_{10}H_{21}$
C_8H_{17}
O
N
O
H
Br
N
Br
N
H
O
N
O
C_8H_{17}
$C_{10}H_{21}$
140
135
130
125
120
115PPM
160
140
120
100
80
60
40
20
PPM

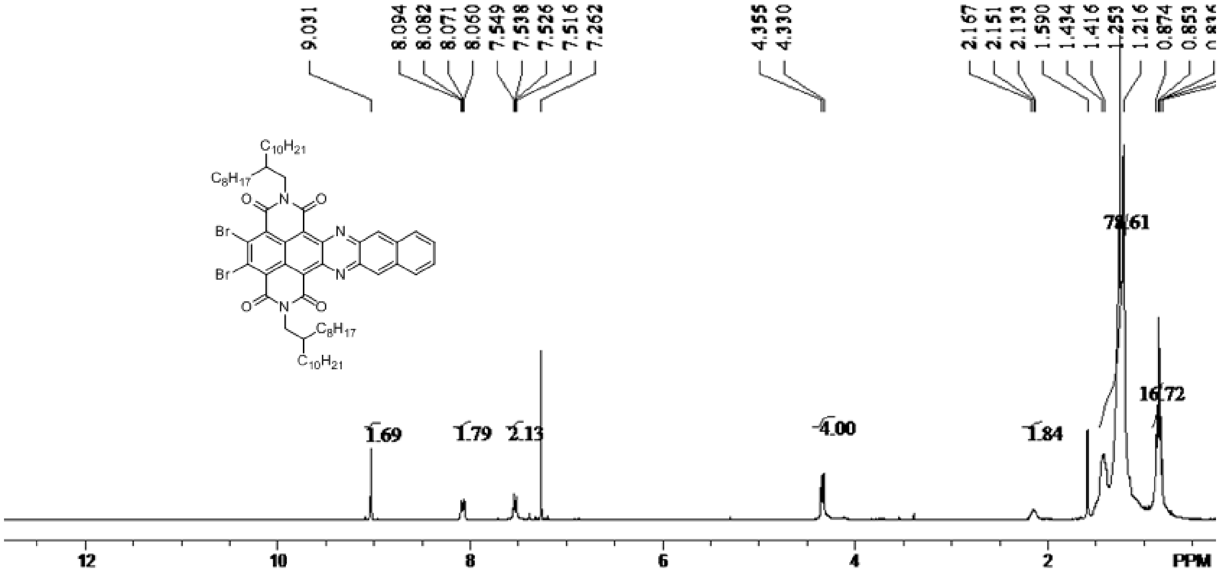
9.031
8.094
8.082
8.071
8.060
7.549
7.538
7.526
7.516
7.262
4.355
4.330
2.167
2.151
2.133
1.590
1.434
1.416
1.253
1.216
0.874
0.853
0.81
$C_{10}H_{21}$
C_8H_{17}
O
N
Br
1.69
1.79
2.13
4.00
1.84
78.61
16.72
12
10
8
6
4
2
PPM

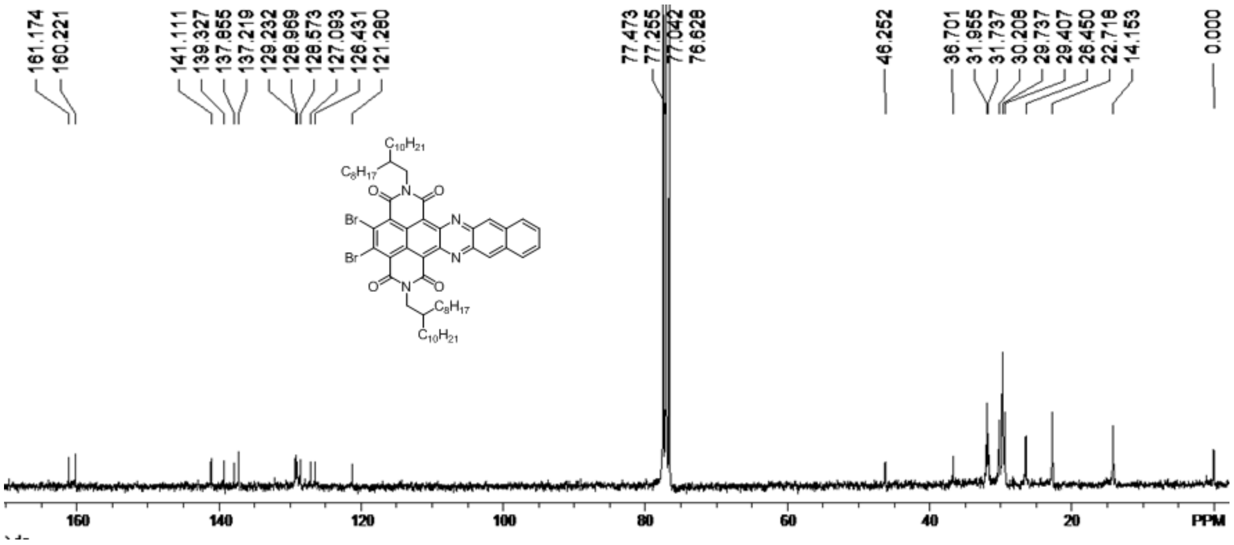
161.174
160.221
141.111
139.327
137.855
137.219
129.232
128.969
128.573
127.093
126.431
121.280
77.473
77.255
77.042
76.828
46.252
36.701
31.955
31.737
30.208
29.737
29.407
26.450
22.716
14.153
0.000
$C_{10}H_{21}$
C_8H_{17}
O
N
Br
160
140
120
100
80
60
40
20
PPM

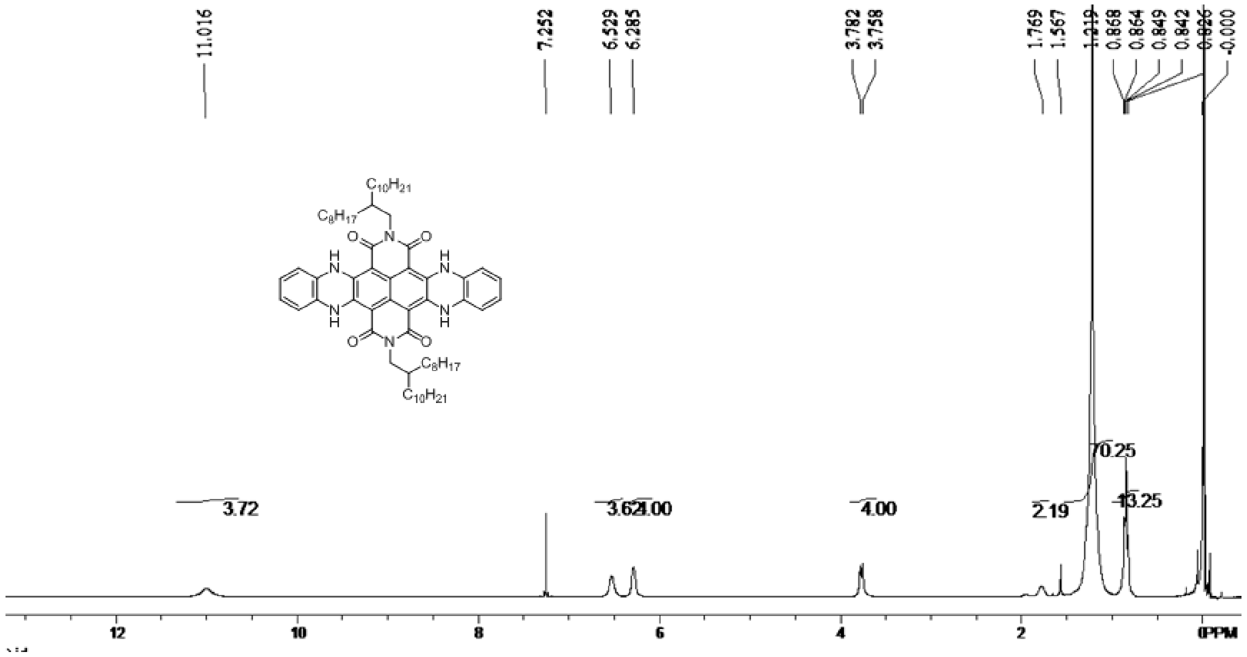
11.016
7.252
6.529
6.285
3.782
3.758
1.769
1.567
1.219
0.868
0.864
0.849
0.842
0.826
-0.000
C10H21
C8H17
O
N
H
3.72
3.62
4.00
4.00
2.19
70.25
13.25
12
10
8
6
4
2
0PPM

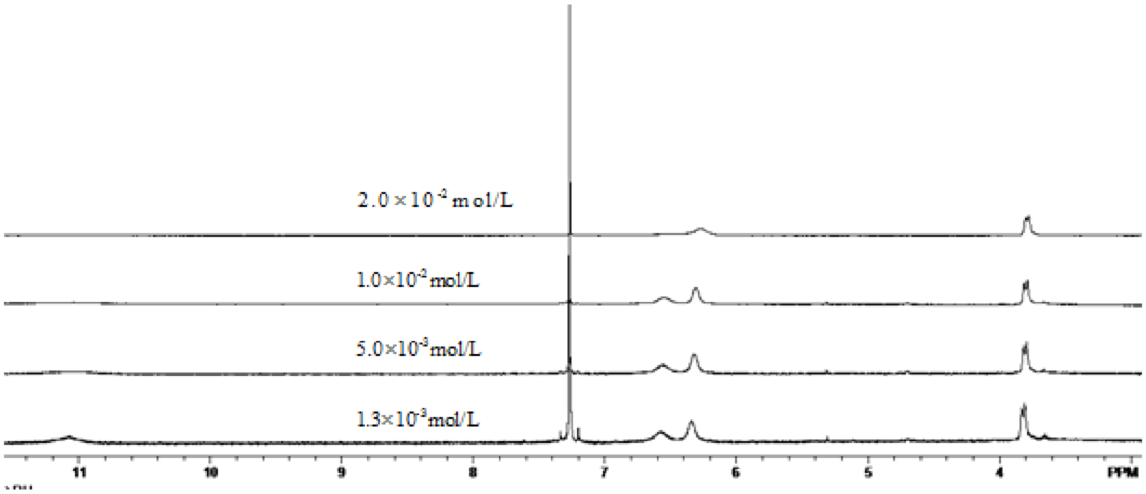
2.0 × 10-2 mol/L
1.0×10-2mol/L
5.0×10-3mol/L
1.3×10-3mol/L
11
10
9
8
7
6
5
4
PPM

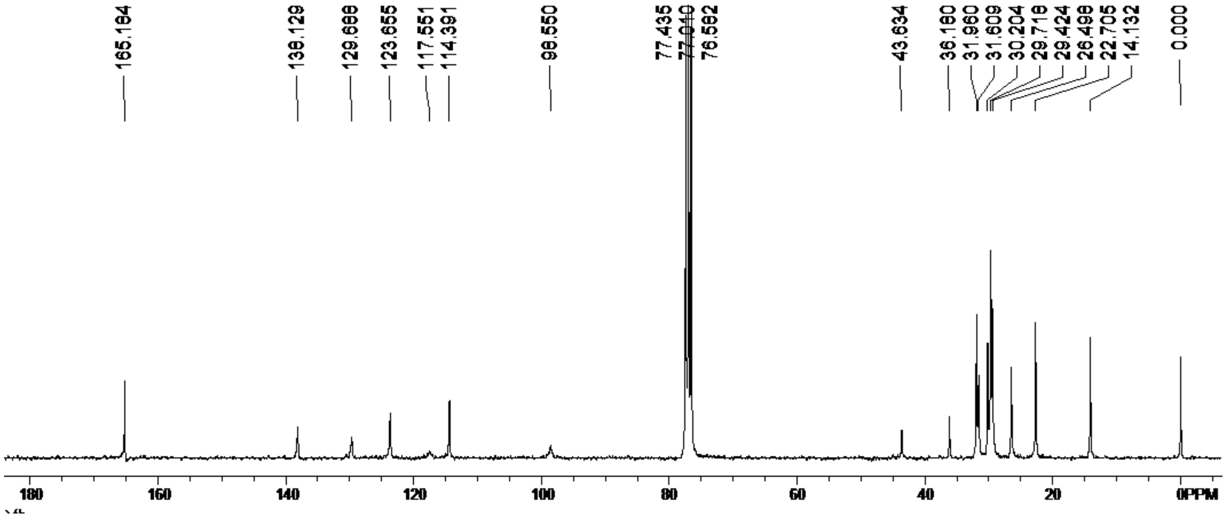
165.164
138.129
129.666
123.655
117.551
114.391
98.550
77.435
77.010
76.582
43.634
36.160
31.960
31.609
30.204
29.716
29.424
26.498
22.705
14.132
0.000
180
160
140
120
100
80
60
40
20
0PPM

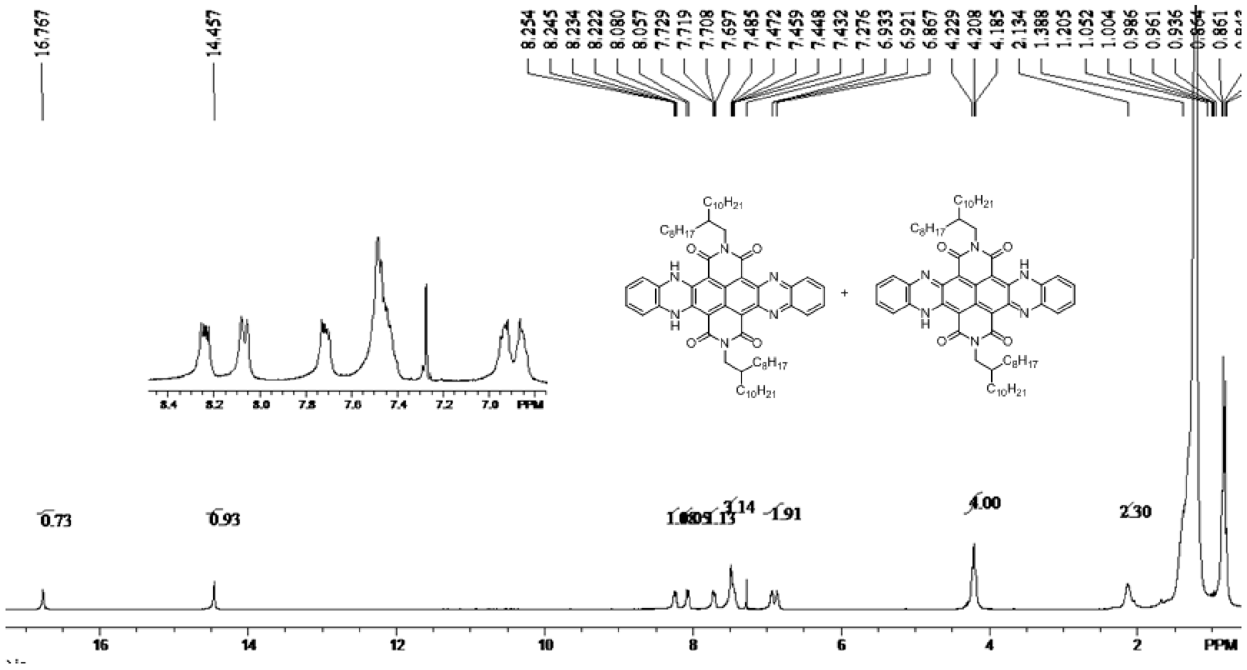
16.767
14.457
8.254
8.245
8.234
8.222
8.080
8.057
7.729
7.719
7.708
7.697
7.485
7.472
7.459
7.448
7.432
7.276
6.933
6.921
6.867
4.229
4.208
4.185
2.134
1.388
1.205
1.052
1.004
0.986
0.961
0.936
0.864
0.861
$C_{10}H_{21}$
C_8H_{17}
+
0.73
0.93
3.14
1.91
4.00
2.30
16
14
12
10
8
6
4
2
PPM
8.4
8.2
8.0
7.8
7.6
7.4
7.2
7.0
PPM

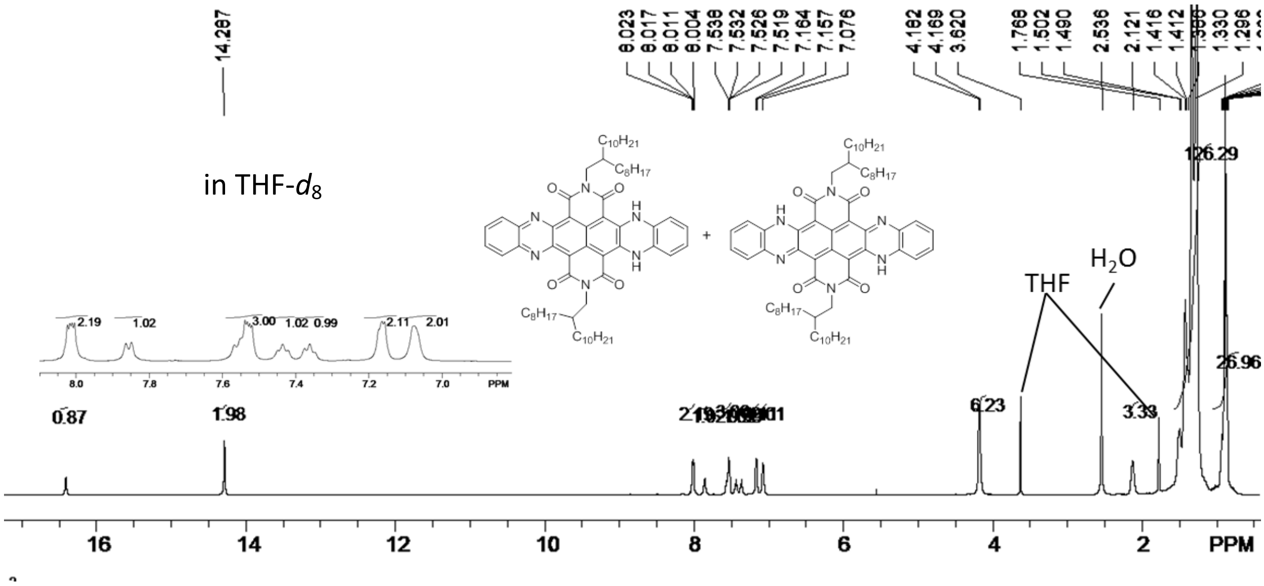
14.287
8.023
8.017
8.011
8.004
7.539
7.532
7.526
7.519
7.164
7.157
7.076
4.182
4.169
3.620
1.769
1.502
1.490
2.536
2.121
1.416
1.412
1.330
1.296
in THF-d_8
$C_{10}H_{21}$
C_8H_{17}
+
THF
H_2O
126.29
26.96
2.19
1.02
3.00
1.02
0.99
2.11
2.01
0.87
1.98
6.23
3.33
16
14
12
10
8
6
4
2
PPM
8.0
7.8
7.6
7.4
7.2
7.0
PPM

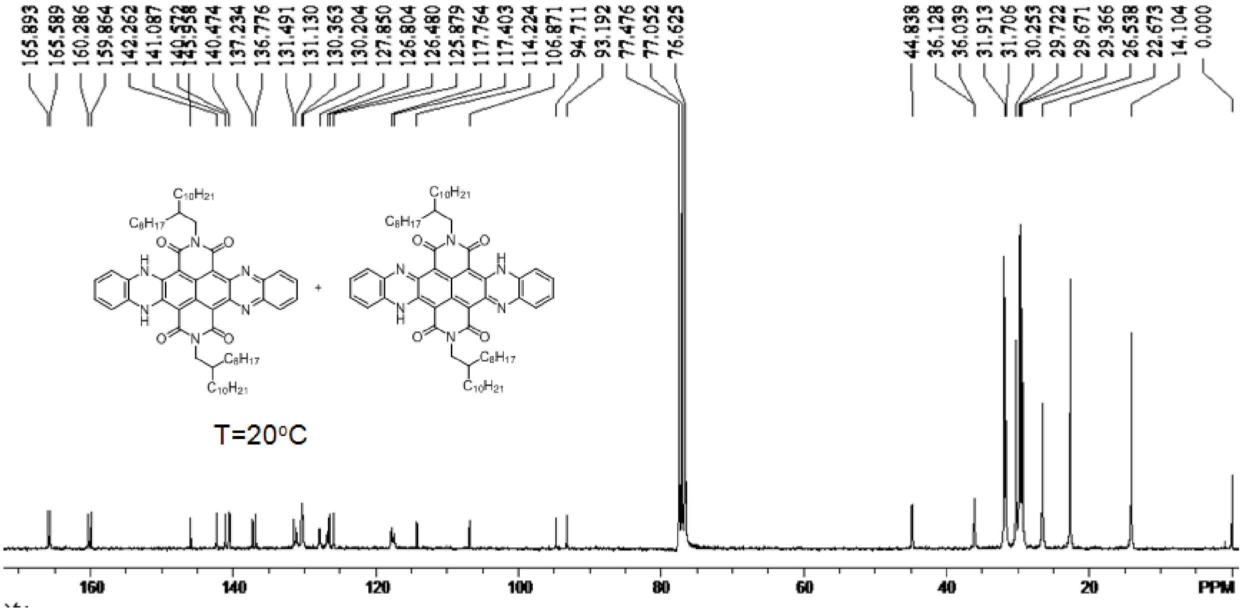
165.893
165.589
160.286
159.864
142.262
141.087
140.474
137.234
136.776
131.491
131.130
130.363
130.204
127.850
126.804
126.480
125.879
117.764
117.403
114.224
106.871
94.711
93.192
77.476
77.052
76.625
44.838
36.128
36.039
31.913
31.706
30.253
29.722
29.671
29.366
26.538
22.673
14.104
0.000
$C_{10}H_{21}$
C_8H_{17}
O
N
H
+
T=20°C
160
140
120
100
80
60
40
20
PPM

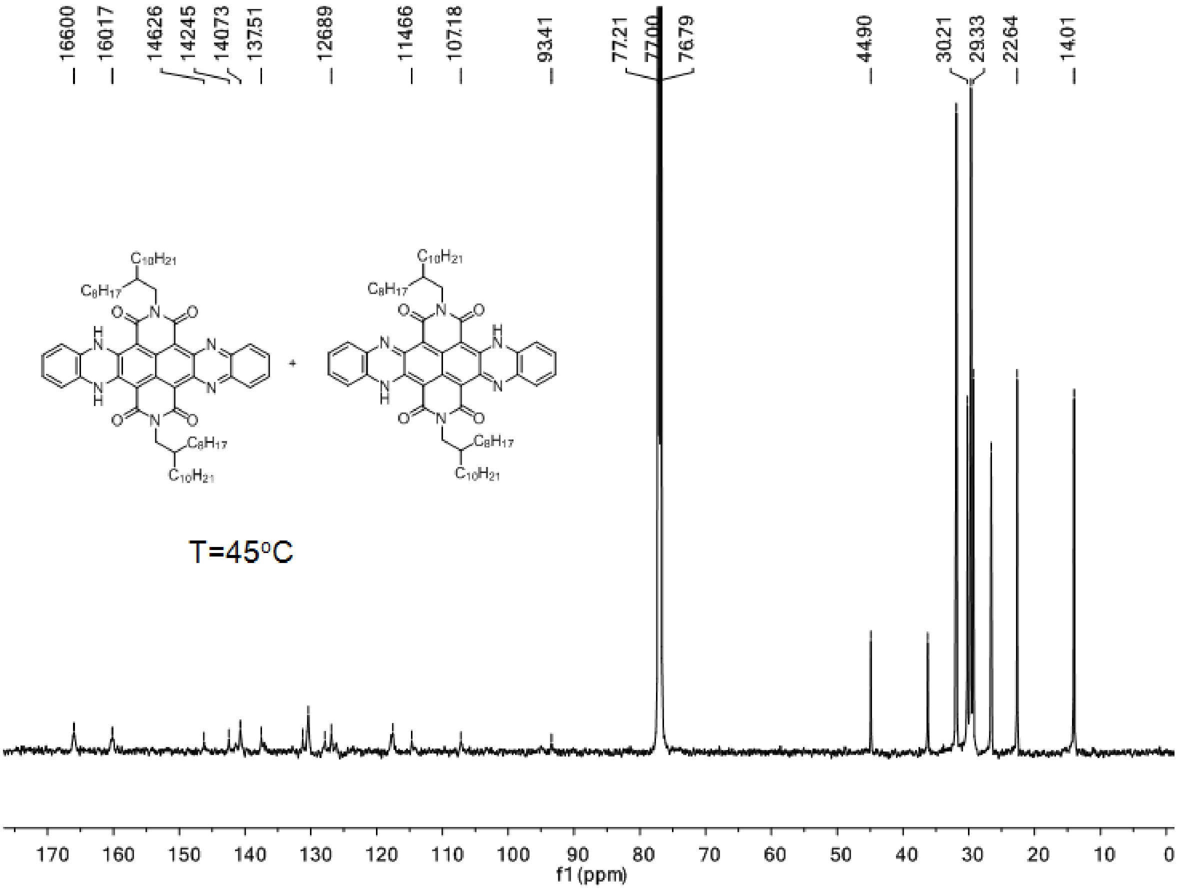
16600
16017
14626
14245
14073
13751
12689
11466
10718
9341
77.21
77.00
76.79
44.90
30.21
29.33
22.64
14.01
$C_{10}H_{21}$
C_8H_{17}
O
N
H
+
T=45°C
170
160
150
140
130
120
110
100
90
80
70
60
50
40
30
20
10
0
f1 (ppm)

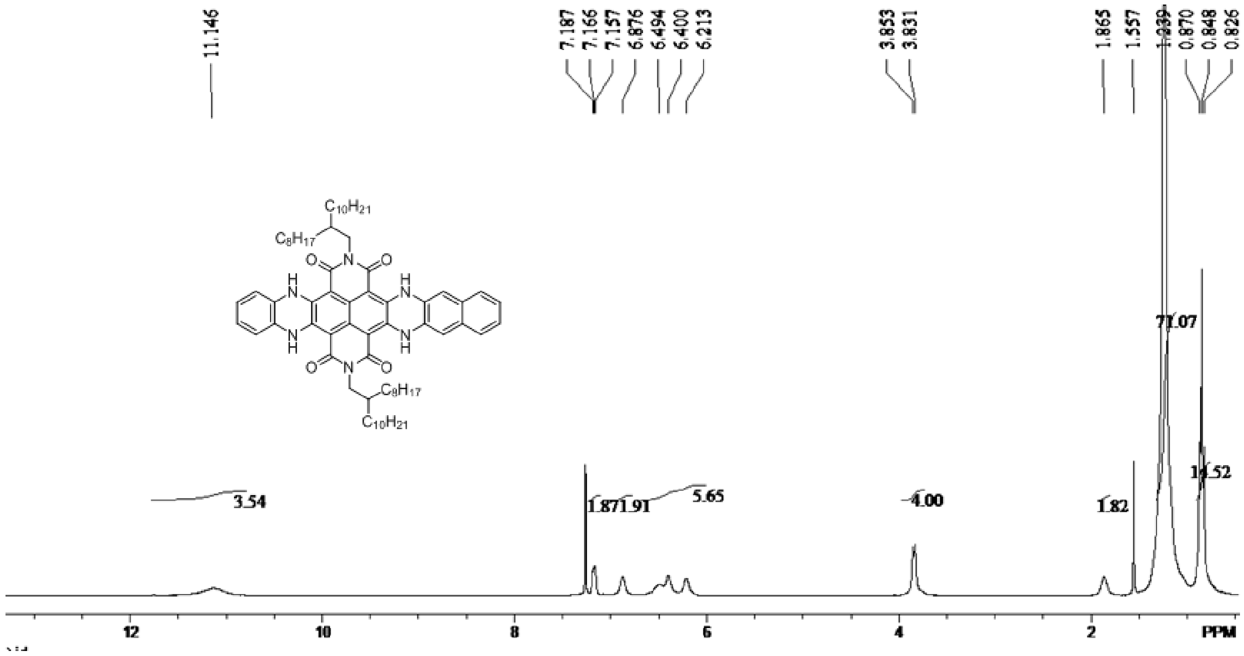
11.146
7.187
7.166
7.157
6.876
6.494
6.400
6.213
3.853
3.831
1.865
1.557
1.239
0.870
0.848
0.826
$C_{10}H_{21}$
C_8H_{17}
O
N
H
C_8H_{17}
$C_{10}H_{21}$
3.54
1.87
1.91
5.65
4.00
1.82
71.07
14.52
12
10
8
6
4
2
PPM

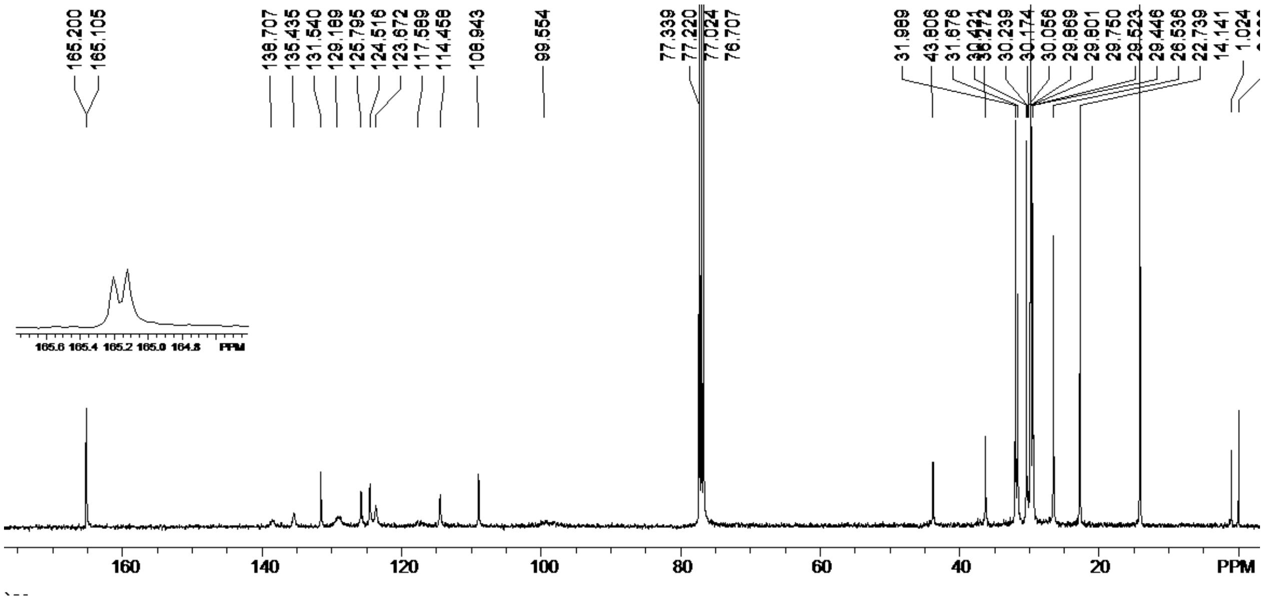
165.200
165.105
138.707
135.435
131.540
129.189
125.795
124.516
123.672
117.589
114.459
108.943
99.554
77.339
77.220
77.024
76.707
31.989
43.606
31.676
30.421
36.272
30.239
30.174
30.056
29.869
29.801
29.750
29.523
29.446
26.536
22.739
14.141
1.024
165.6
165.4
165.2
165.0
164.8
PPM
160
140
120
100
80
60
40
20
PPM

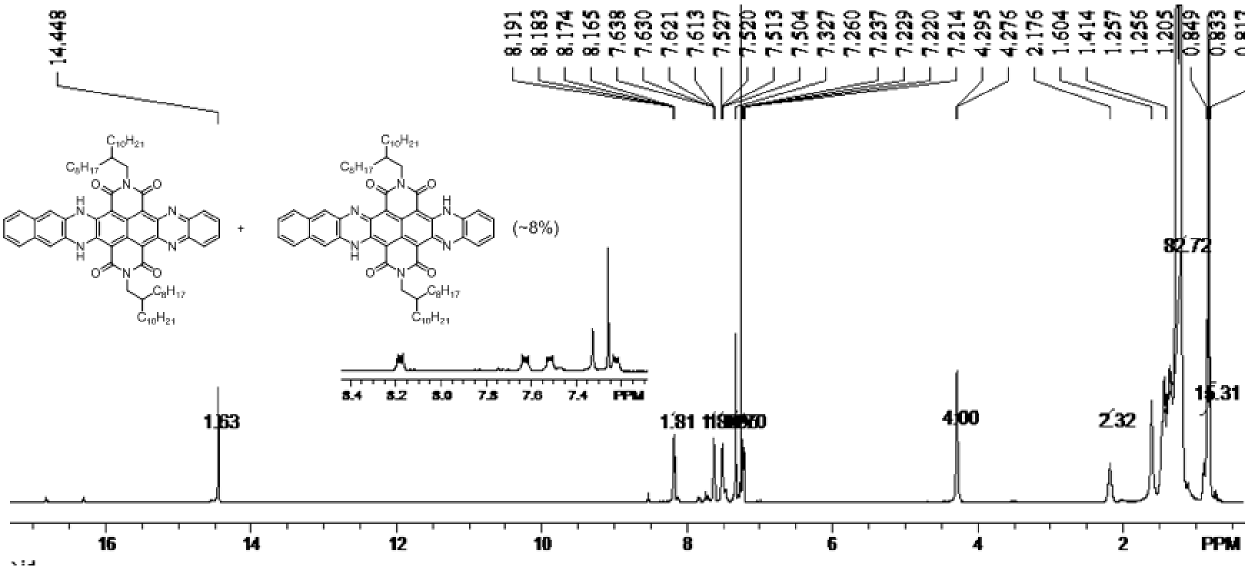
14.448
8.191
8.183
8.174
8.165
7.638
7.630
7.621
7.613
7.527
7.520
7.513
7.504
7.327
7.260
7.237
7.229
7.220
7.214
4.295
4.276
2.176
1.604
1.414
1.257
1.256
1.205
0.849
0.833
$C_{10}H_{21}$
C_8H_{17}
+
(~8%)
1.63
1.81
4.00
2.32
82.72
15.31
16
14
12
10
8
6
4
2
PPM
8.4
8.2
8.0
7.8
7.6
7.4
PPM